

Swimming strategy of settling elongated micro-swimmers by reinforcement learning

Jingran Qiu¹, Lihao Zhao^{1,2†}, Chunxiao Xu¹ and Yichen Yao¹

¹AML, Department of Engineering Mechanics, Tsinghua University, 100084 Beijing, China

²Department of Energy and Process Engineering, Norwegian University of Science and Technology, 7491 Trondheim, Norway

(Received xx; revised xx; accepted xx)

Motile microorganisms in aquatic ecosystems are able to sense the changing surrounding environment and can adjust their motion accordingly to reach certain regions that are favourable for their growth or reproduction. Studying the moving strategies of microorganisms is of great importance for an in-depth understanding of their behaviour in aquatic environment. In present work, we model microorganisms as smart swimming particles and introduce reinforcement learning approach to investigate the strategy for moving upward in a two-dimensional flow field. We explore for the first time how gravity and elongation of a particle affect the strategies obtained by reinforcement learning and compared with the cases of naive gyrotactic particles. We examine the micro-swimmers with different motilities (quick-alignment and slow-alignment). Interestingly, under the same conditions of quick-alignment motility and flow configuration multi-solutions of swimming strategy are observed in the case of smart particles trained by reinforcement learning. However, the multi-solutions are converged into an almost optimal strategy with inclusion of gravity, which acts as a constraint on particle motion. Moreover, the elongation of particle is found to enhance the ability of particle in sampling the low vorticity and upwelling region, which is beneficial for the particles to achieve the given goal. When the settling and elongation are both considered for the particles with slow-alignment motility, similar performance of moving upward is observed for both smart and naive particles. The interesting findings indicate that the diversity of proper strategies is restricted with including constraints of more realistic factors and we suspect that the elongation and gyotaxis of microorganism might be an almost optimal strategy for swimming upwards against gravity after the long term evolution through natural selection. Additionally, the current work on the swimming strategies of more realistic particles reveals the effectiveness of reinforcement learning approach in the study of the behaviour of microorganisms in fluid flow.

Key words: Keywords

1. Introduction

Microorganisms are ubiquitous in environment. In aquatic ecosystem, planktons, such as micro algae and bacteria, are typical examples. The passive microorganisms just float with the fluid while the active ones, however, can swim and adjust their motion with the help of special cellular structure, for instance, flagella (Blair 1995; Drescher *et al.* 2009).

† Email address for correspondence: zhaolihao@tsinghua.edu.cn

How the swimming motion affects the distribution or deposition of microorganisms in the flow has been an intriguing question. Active microorganisms are normally modelled as swimming particles, which can swim and rotate themselves towards a specific direction (Kessler 1986*b*; Pedley & Kessler 1987). Most of the earlier studies have been focusing on so-called naive particle model, in which the particles were supposed to be motile but unable to sense and react with the changing flow environment. Gyrotactic particle, for example, adjusts its alignment by a gravitational torque induced by the inhomogeneous density distribution (Kessler 1986*b*). The motion and deposition of gyrotactic particles have been studied both in laminar (Bearon *et al.* 2011; Durham *et al.* 2009, 2011; Kessler 1985; Thorn & Bearon 2010) and turbulent flows (Bearon *et al.* 2011; De Lillo *et al.* 2014; Santamaria *et al.* 2014; Croze *et al.* 2013; Zhan *et al.* 2014). These results showed that the motion and clustering patterns of particles are altered due to the presence of swimming velocity and gyrotaxis. However, it has been discovered that microorganisms in realistic flow environment can perceive local information, such as temperature (Tawada & Miyamoto 1973; Poff & Skokut 1977), light intensity (Kessler 1986*a*; Garcia *et al.* 2013) or flow motion and acceleration (Fuchs *et al.* 2013, 2015; Sengupta *et al.* 2017), and adjust their motion to reach the locations that are favourable to their growth and reproduction. Studying the strategy of how microorganisms react with flow environment is of great importance for advancing our understanding of their habits and the physics of particle-fluid flow interaction, which may be helpful for the design of micro motile robots to carry out specific tasks.

Recently, some studies have been reported about utilizing machine learning approach to investigate the behavioural strategies of animals in fluids. Novati *et al.* (2017) studied the optimal swimming behaviour of a fish that follows another fish. The result shows that reinforcement learning approach successfully provides an optimized swimming strategy for the following fish to make use of the leader's wake, reducing drag and thus saving energy. Gazzola *et al.* (2016) presented an investigation on schooling of fish to minimize the energy consumption of individuals based on the hydrodynamic environment. Similar research on birds or gliders soaring in turbulence is performed by Reddy *et al.* (2016), revealing the effectiveness of machine learning in obtaining proper strategies to control the motion of a glider. Back to the works about active particles, some studies were recently conducted on the swimming strategy of *smart* active particles, which can perceive the local flow information and adjust their motion to achieve given goals (Colabrese *et al.* 2017; Gustavsson *et al.* 2017; Colabrese *et al.* 2018). These studies successfully reached almost optimal strategies by reinforcement learning approach and showed the great potential of this novel numerical approach. The pioneer work on the above-mentioned subject was presented by Colabrese *et al.* (2017), who considered point-like, inertial-less spheres in a two-dimensional stationary *Taylor-Green vortex flow* (TGV). They assumed that smart particles can perceive local flow direction and vorticity and swim with a constant velocity in a direction that a smart particle can actively orientate itself to. A simple goal given to these particles is that they need to swim upwards as fast as possible, and the reinforcement learning approach was adopted for training the particles to obtain optimal swimming strategies. Particles with different swimming velocity and responding time of the preferential alignment were tested and the results show that smart particles perform much better than naive ones. Another relevant work extended the analysis to a more complex flow configuration: a three-dimensional chaotic *ABC flow* (Gustavsson *et al.* 2017). A satisfying outcome was reached that the trained smart particles can avoid vortexes trapping and find proper regions where they can swim upwards faster by the help of upwelling flow. These two works mentioned above have been both focusing on rigid inertial-less spherical particles. Colabrese *et al.* (2018) recently applied reinforcement

learning on inertial spherical particles which can actively adjust their volume while keeping mass constant. Therefore, the particles can control their density, heavier or lighter than the flow, and then being thrown away or attracted in a vortex. The goal of a particle is to sample a specific flow region which is artificially given in advance. In particular, particles in a two-dimensional TGV-like flow or three-dimensional ABC flow can sense the local vorticity and control their density to adjust their motion, finally reaching the target region. Unsteady flow was considered in this paper, and the result showed that smart particles outperform naive ones in most cases. This proves the effectiveness of reinforcement learning algorithm in relatively complex configurations, unsteady and three-dimensional flow, for instance.

The earlier studies suggest that smart particles trained by reinforcement learning can capture the characteristics of background flow and reach an approximately optimized strategy for the given goals. Nevertheless, all these studies focused on relatively simple particle models, which only considered spherical particle and excluded the gravity effect. It is well known that, in nature, microorganisms have a variety of shape and some of them are subject to the influence of gravity. Hence, some open questions remain unanswered behind the aforementioned studies: does reinforcement learning still work when gravity and shape of particles are taken into consideration? What is the influence of gravity and particle shape on the effectiveness of swimming strategy? Would the smart particle adopt different strategies with inclusion of sedimentation and asphericity? Would smart particle always perform better than naive gyrotactic particle? Another issue we are interested in is about the algorithm itself. The earlier works showed that reinforcement learning approach require normally thousands of iterations to train an individual particle to reach a converged strategy. Is it possible to accelerate the process by training hundreds of particles in parallel to greatly reduce the computation time? This might be vital when we apply the approach into a relatively complex flow configuration, such as particles in turbulence, where heavy cost of computation in every iteration would hinder the feasibility of this approach.

To address the above questions, we investigate the influences of gravitational sedimentation and particle shape on swimming strategies of tracer elongated particles in a two-dimensional stationary Taylor-Green vortex flow. Moreover, we put forward an improvement of the algorithm of reinforcement learning to accelerate the training process. In Section 2, we firstly introduce the model of settling elongated spheroid and followed by the reinforcement learning algorithm. Section 3 presents the results of the gravity and shape effects on swimming strategies of *quick-alignment* and *slow-alignment* particles. Finally, we draw the conclusions in Section 4.

2. Methodology

2.1. Governing equations

In present work, we model micro-swimmers as tracer particles with consideration of settling caused by gravity. Particles are small relative to the characteristic length scale of the flow and their density is close to that of the fluid. The parameters are given in table 1 and 2 and, accordingly, the tracer particle model can be justified in present work. However, settling velocity is unneglectable relative to swimming velocity so that we introduce the Stokes settling velocity to take the effect of gravity into account. The particle translational motion is governed by the following equation:

$$\dot{\mathbf{x}} = \mathbf{u}|_p + v_{swim}\mathbf{p} + \mathbf{v}_s + \sqrt{2D_t}\boldsymbol{\eta}, \quad (2.1)$$

where \mathbf{x} and $\mathbf{u}|_p$ are the particle position and local fluid velocity at particle location, respectively. The swimming velocity is of constant magnitude v_{swim} in the direction of particle orientation \mathbf{p} to model the microorganism that swims with a constant velocity relative to the fluid motion (Pedley & Kessler 1992). D_t is the dissipation rate of particle translation, and $\boldsymbol{\eta}$ is a white Gaussian noise vector for simulating the dissipation in two directions. Settling velocity \mathbf{v}_s , scaling the influence of gravitational sedimentation (Niazi Ardekani *et al.* 2017), is defined as follows:

$$\mathbf{v}_s = v_{settle} \left(\frac{\pi}{2} \right) \mathbf{e} + \left(v_{settle}(0) - v_{settle} \left(\frac{\pi}{2} \right) \right) (\mathbf{e} \cdot \mathbf{p}) \mathbf{p}, \quad (2.2)$$

where \mathbf{e} is the direction of gravity and $v_{settle}(\theta_g)$ is the settling velocity of a spheroid particle in a quiescent flow with a fixed angle θ_g between particle major axis and gravity direction, which is given by

$$v_{settle}(\theta_g) = 6\pi a \lambda \left(\frac{1}{(k_{\hat{z}\hat{z}} - k_{\hat{x}\hat{x}}) \cos^2 \theta_g + k_{\hat{x}\hat{x}}} \right) \frac{2Da^2 g}{9\nu}. \quad (2.3)$$

$k_{\hat{x}\hat{x}}$ and $k_{\hat{z}\hat{z}}$ are the components of resistant tensor of a spheroid (Siewert *et al.* 2014). a , g and ν are semi-minor axis of spheroid, gravitational acceleration and kinematic viscosity of fluid, respectively. D is the relative difference between particle density ρ_p and fluid density ρ_f , defined by

$$D = \frac{\rho_p - \rho_f}{\rho_f}. \quad (2.4)$$

One can refer to figure 1 for a more intuitive comprehension of particle motion. Note that the settling velocity is not always aligned in the gravity direction. It depends on the direction of instantaneous orientation \mathbf{p} , which is governed by

$$\dot{\mathbf{p}} = \frac{1}{2B} [\mathbf{k} - (\mathbf{k} \cdot \mathbf{p}) \mathbf{p}] + \frac{1}{2} \boldsymbol{\omega} \times \mathbf{p} + \frac{\lambda^2 - 1}{\lambda^2 + 1} [\mathbf{I} - \mathbf{p}\mathbf{p}] \mathbf{S}\mathbf{p} + \sqrt{2D_R} \boldsymbol{\xi}. \quad (2.5)$$

\mathbf{p} is the orientation vector in the inertial frame. On the right hand side, the first term represents the effect of particle active alignment. \mathbf{k} is a unit vector in the direction of the preferential orientation of a particle. For naive gyrotactic particles, \mathbf{k} is constantly opposite to gravity direction. B is the characteristic timescale of particle active alignment, scaling the ability of rotating back to the active alignment. The second and third term denote the contribution of fluid vorticity and deformation rate, respectively. $\boldsymbol{\omega}$ is the fluid vorticity at particle position, and \mathbf{S} is the local deformation rate tensor. $\lambda = a/c$ is the aspect ratio of a particle, denotes the ratio of major and minor axis of a spheroid. For non-spherical particles, the effect of fluid deformation must be considered, and it may even dominate the particle orientation when aspect ratio is much larger than one. The last term is to simulate the dissipation of rotation, as that of translation in equation 2.1. D_r and $\boldsymbol{\xi}$ are the dissipation rate of particle rotation and a vector of white Gaussian noise, respectively.

In present study, we consider smart or naive spheroidal particles swimming in a Taylor-Green vortex flow. The two-dimensional steady flow is given by:

Parameter	Symbol	Value
length scale of flow	L_0	1×10^{-2} m
characteristic velocity of flow	u_0	1×10^{-3} m/s
density ratio	ρ_p/ρ_f	1.05
kinematic viscosity of fluid	ν	1×10^{-6} m ² /s
gravitational acceleration	g	9.8m/s ²

TABLE 1. Flow parameters

Parameters	quick-alignment		slow-alignment					
λ	1	1	1	2	3	5	10	20
$a(\mu\text{m})$	31.62	21.43	31.62	25.64	23.13	20.67	18.23	17.13
$v_s^{iso}(\mu\text{m/s})$	108.9	50.0	108.9	108.9	108.9	108.9	108.9	108.9
$v_{swim}(\mu\text{m/s})$	300	100	300	300	300	300	300	300
$B(\text{s}^{-1})$	1.5	1.5	50	50	50	50	50	50

TABLE 2. Particle parameters

$$\begin{cases} u_x = \frac{u_0}{2} \cos \frac{x}{L_0} \sin \frac{y}{L_0}, & (2.6) \\ u_y = -\frac{u_0}{2} \sin \frac{x}{L_0} \cos \frac{y}{L_0}, & (2.7) \\ \omega_z = -\frac{u_0}{L_0} \cos \frac{x}{L_0} \cos \frac{y}{L_0}. & (2.8) \end{cases}$$

u_x , u_y and ω_z are the flow velocity in x and y direction and the vorticity, respectively. u_0 and L_0 are the characteristic velocity and length of the flow, and the detailed value of parameters can be referred to in table 1. The flow is spatially periodic and particle motion and orientation are constrained in x - y plane. The position of a particle is restricted in a finite region by periodic boundary conditions. The swimmers aspect ratio λ is ranging from 1 to 20 (see table 2) to examine the shape effect of particles. v_s^{iso} is the mean settling velocity of randomly-oriented particles in a quiescent flow. Settling velocity is controlled at a constant level to exclude the influence of aspect ratio on settling velocity. The parameters of particles are chosen to match a swimming micro-cell (Kessler 1986*b*).

2.2. Reinforcement learning approach

In present study, we adopted *one-step Q-learning*, one of the algorithms of reinforcement learning, to train smart particles to swim upwards in a given flow. The particle is assumed able to sense and perceive the information of environment and thus determines the state s . Then the particle selects a preferential action a based on the state according to the current strategy Q . Specifically, all probable states are divided into finite numbers of intervals (s_1, s_2, \dots, s_n) and a Q table $Q(s, a)$ stores the value of every possible pair of state-action. In current model, the state space is the combination of four possible local flow directions (i.e. down, right, up and left) and three possible vorticity levels (i.e. positive, negative and approximately zero). Particles possible action is selected within four options (orientating down, right, up or left). Thus, the Q table is a 12×4 matrix

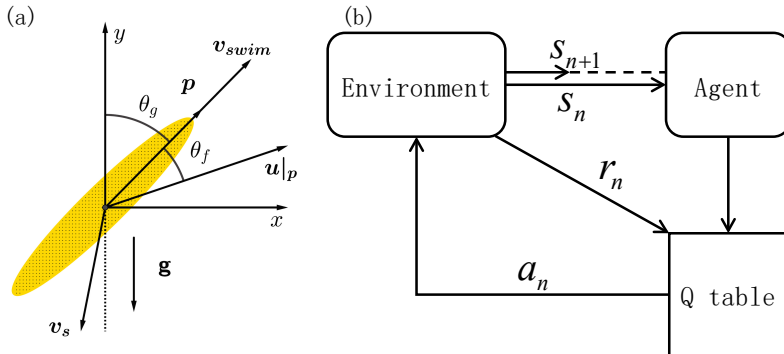


FIGURE 1. (a) A sketch of an elongated particle in x-y plane. v_{swim} , $u|_p$ and v_s denote the swimming velocity, fluid velocity at particle position and settling velocity, respectively. The velocity of a particle in the inertial frame is the summation of these three velocities. (b) A flow chart of the training process of one-step Q-learning approach. Agent represents the particles in present study and environment represents the background flow.

determining swimming strategy for smart particles. As long as the model of particle sensing and acting is well defined, the remaining task is to train an optimal Q table through reinforcement learning approach.

The training procedure is described in a flow chart (figure 1b). Initially, particles are randomly released in the flow field and they will then swim and rotate, while perceiving local flow information to determine the states at every time step. When the n^{th} state change occurs, particle will select an action a_n based on Q table according to the current states s_n . At the following time steps after particle has made an action, once it reaches a new state s_{n+1} a reward r_n will be calculated. In specific, the reward is defined as the vertical distance the particle travels between two state changes. Accordingly, we modify the value of corresponding elements of Q table using the following equation,

$$Q(s_n, a_n) = Q(s_n, a_n) + \alpha \left[r_{n+1} + \gamma \max_a (Q(s_{n+1}, a) - Q(s_n, a_n)) \right], \quad (2.9)$$

where α is the learning rate, which can be manually adjusted to control the convergence rate. γ is the discount rate with $0 < \gamma < 1$, determining how far-sighted the strategy is. Specifically, γ is 0.999 in present study, indicating most of the future reward will be taken into consideration, and a far-sighted strategy will be obtained. Equation 2.9 is an approximation iteration to reach an optimal Q table for a value iteration of Markov Decision Process (MDP) (Sutton & Barto 1998). One will converge on the optimal strategy only with the premise that the particle experiences every state and take every action for infinite times. In practice, the convergence of an approximately optimal strategy can be achieved as long as a particle experiences sufficient tries of different states and actions. Therefore, the training process is divided into several episodes, where one hundred particles will be initially randomly located and orientated to promote different tries of possibility. Particles move in the flow for a fixed number of time steps and update the Q table according equation 2.9, and the Q table converges on an approximately optimal strategy after enough number of episodes.

In order to evaluate the effectiveness of training process, we introduce average gain defined as followed:

$$\Sigma(E) = \frac{\bar{v}_{y,smart} - v_s^{iso}}{\bar{v}_{y,naive} - v_s^{iso}}, \quad (2.10)$$

where $\bar{v}_{y,smart}$, $\bar{v}_{y,naive}$ and v_s^{iso} are the averaged vertical velocity of smart and naive particles and the mean settling velocity in one episode, respectively. Regarding the case without gravity, v_s^{iso} is zero. The average gain represents the mean vertical smart particle velocity compared to naive ones. It is intuitionistic that $\Sigma(E)$ is greater than 1 when smart particles outperform naive ones. Note that the average gain is relevant to the total time of simulation, for the decrease of the average \bar{v}_y occurring when particles are gradually trapped in vortex. Therefore, the comparison of average gain is based on the same length of time.

According to the earlier studies (Colabrese *et al.* 2017; Gustavsson *et al.* 2017; Colabrese *et al.* 2018), only one particle is simulated in the training process, which is convenient for tracking the learning gain. However, another problem is raised that a large number of episodes is needed for training a single particle. Considering the relatively slow motion of particle in the flow, states are expected to be changed slowly in the simulation and, therefore, the frequency of updating Q table is restricted. As a result, a large number of episodes is often needed. To reduce the number of episode, we choose to train multiple particles in one episode simultaneously, which enhances the frequency of updating Q table for a faster convergence and allows particles to explore more probability in one episode. By selecting suitable particle number and learning rate, we can greatly reduce the number of episodes and improve the efficiency of training process. This might be vital in the case of more complex flow configurations, such as in turbulent flows. A detailed discussion is given in Appendix I.

3. Results and Discussion

In this section, we consider two types of particles in a TGV flow with application of reinforcement learning approach. The first type of particles can align to the active orientation quickly and, therefore, are named as *quick-alignment* particles. The other type of particles ability of active alignment is relatively slower and, therefore, more easily to be affected by the flow. Thus, they are called *slow-alignment* particles. The characteristic timescale of active alignment B is used to distinguish the two types of particles. More specifically, the quick-alignment particles have smaller B .

3.1. Quick-alignment particles

We firstly consider the case of spherical particles with $v_{swim} = 0.3u_0$, $B = 0.15L_0/u_0$ and $v_s^{iso} = 0.1089u_0$. Because of the small B , particle orientation is dominated by the active orientation. We implement the reinforcement learning in the cases with and without the inclusion of gravity. Figure 2 shows the result of average gain in the training procedure (a, b) and a series of typical patterns of smart particles swimming trajectories (c-f). In the cases without gravity, three different patterns of swimming strategies are obtained, which indicates that multi-solutions of strategy are given by reinforcement learning. These strategies have different levels of averaged gain in accordance with the different swimming trajectories of particles, as shown in figure 2. The first type of strategy with the highest averaged gain is shown in figure 2c, in which particles move upwards along a winding *S-shaped* track to avoid the traps of vortex. Particles orientate upwards in most of time (figure 3a) and, therefore, move in the S-shaped track carried by the flow. Thus, three peaks at $\theta_f = -\pi/2, 0$ and $\pi/2$ are observed in figure 3b, corresponding to the

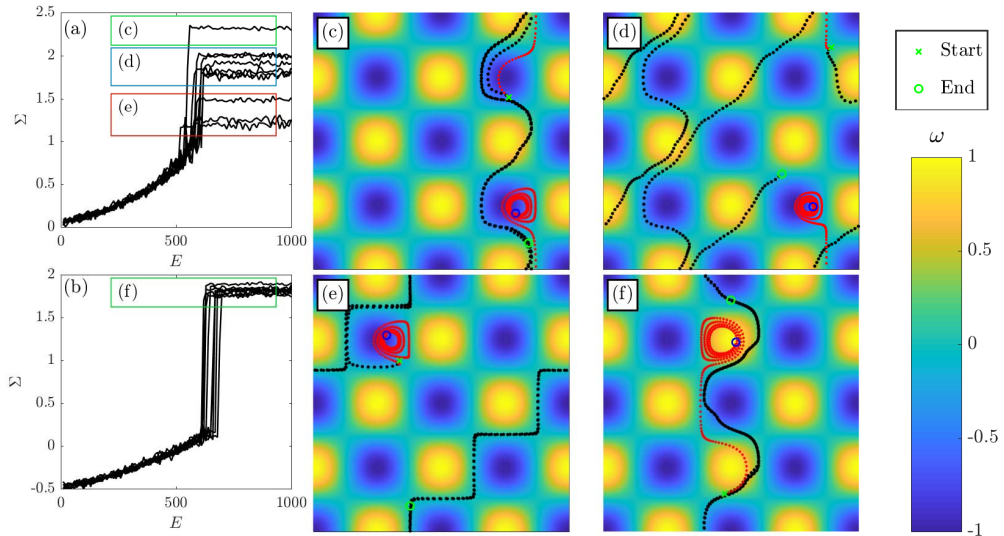


FIGURE 2. The average gains in separated training of spherical particles. (a) Non-settling particles; (b) Settling particles. The box marked with the panel number corresponds to the representative trajectories on the right. (c-e) The typical trajectories of spherical non-settling particles in a $4\pi \times 4\pi$ domain, and (f) that of settling particles. In panel (c-f), black dots represent smart particles while red dots represent naive ones. The background is coloured by fluid vorticity.

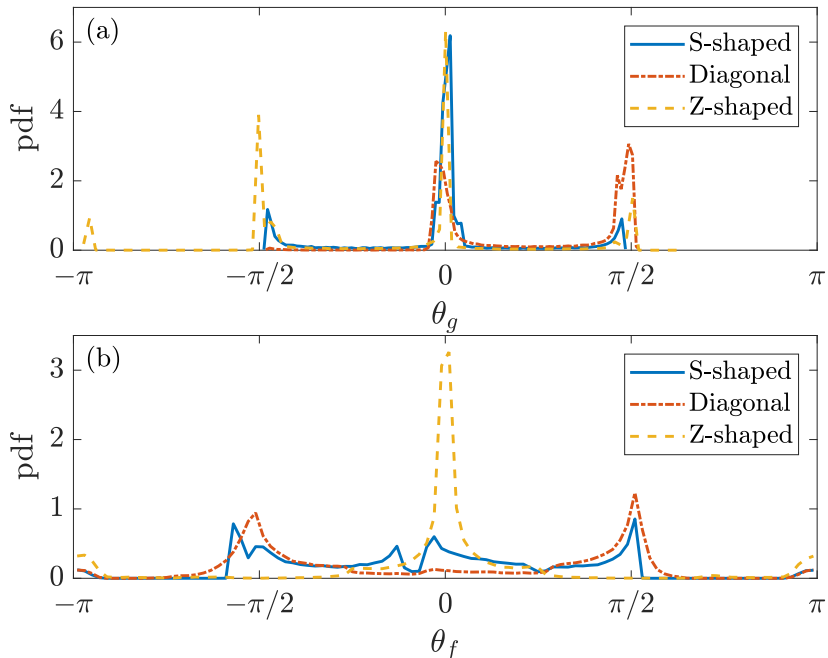


FIGURE 3. Probability density function of (a) the angle θ_g between particle orientation and vertical direction, and (b) the angle θ_f between particle orientation and local flow direction.

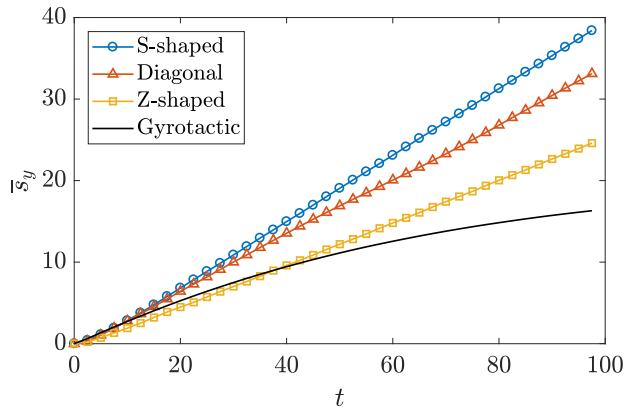


FIGURE 4. Averaged vertical displacement of particles \bar{s}_y as a function of time.

particles in leftward flow (e.g. under a negative vortex), in upwelling flow (e.g. in the left of a negative vortex) and rightward flow (e.g. over a negative vortex), respectively. The type of strategy with second highest averaged gain is shown in figure 2d, where particles move on a *diagonal* track. This observation is in agreement with the result of previous works (Durham *et al.* 2011; Colabrese *et al.* 2017). Specifically, most of the smart particles align upwards or leftwards (figure 3a), and their orientations are perpendicular to local fluid velocity (figure 3b), which means that smart particles align upwards when the local fluid velocity is vertical but align horizontally when the flow is upwelling. The last type of strategy is shown in figure 2e, where particles cluster at low vorticity region and move on a *Z-shaped* track. Most of particles align vertically or horizontally, swimming along the local flow direction (figure 3). Figure 4 shows the comparison of averaged vertical displacement of three types of strategies. The S-shaped strategy performs the best for particles swimming upwards in most of time, while Z-shaped strategy performs the worst for the longest route and spending time swimming horizontally. In spite of that, all three types of strategies can help particles continuously swim upwards, which thus have better performance than gyrotactic naive particles that are preferentially trapped inside vortices.

However, with inclusion of gravity, three different patterns of swimming strategy are converged into the same pattern with S-shaped winding trajectories (see figure 2b and f), which is similar to the best-performing strategy of non-settling cases. One possible explanation of the convergence into a better strategy is that the effect of gravity confines the range of proper sub-optimal strategies. Here, settling velocity is set to be significant relative to the swimming velocity (about 36% of swimming velocity). When gravity is applied, particles need to swim against the gravity and otherwise they might fall into a vortex and get trapped. Therefore, the strategy obtained in no-gravity case might be no longer suitable for the settling case. For instance, the Z-shaped strategy that mentioned above is no longer stable when particles keep settling down, for a particle being difficult to keep on a same height when swimming horizontally. It seems that when more constraints are enforced on the particle motion, a stronger convergence of strategies might be given by reinforcement learning approach.

To further examine the aforementioned assumption, particles with smaller swimming velocity are considered with $v_{swim} = 0.1$, $B = 0.15L_0/u_0$ and $v_s^{iso} = 0.05u_0$. Similarly, particles are trained in non-settling and settling cases. Since the swimming velocity of particles are reduced, the motion of particles is further confined. Therefore, only S-shaped strategies are obtained in non-settling cases according with the results by Colabrese *et al.*

(2017) and also in settling cases which are not considered in that work. Although the strategies in both cases lead particles swimming along similar trajectories (figure 5), differences of actions can be found in specific regions of the flow. The background flow goes downwards in the right of a negative vortex or in the left of a positive vortex, and these regions are so called downwelling regions. Since downwelling flow carries particles downwards, it is an unprofitable region for particles with the goal of moving upwards as fast as possible. Therefore, particle's choice of swimming direction in downwelling flow may have great influences on the rewards and the performance of a strategy. In non-settling case, particles choose to swim upwards in some of the strategies obtained in separated training (figure 5a) and choose to swim downwards in others (not shown). Regardless of the swimming direction, the performances of these strategies are at the same level, because of the low possibility of a particle moving into downwelling regions on a stable S-shaped track. However, when gravity is applied, the diversity of strategies diminishes. Particles might fall into the downward flow because of settlement, especially when they move near the stagnation point of the flow. The particles could be easily trapped by vortexes if they still try to swim upwards against the flow. For settling particles, swimming downwards is a better choice in downwelling regions. In spite of temporary negative reward, swimming straight downwards can help particles get out of the unprofitable regions quickly, and then move back on the path of lifting, which has a higher long-term reward. Therefore, smart particles learn to swim downwards in all strategies when settling is considered (figure 5b). This is also an exemplification of the assumption that constraint could confine the possible optimal strategies. Moreover, it is interesting to see how particles learn to swim downwards temperately to reach a higher long-term goal, indicating that particles might be able to extract the feature of background flow through reinforcement learning.

The shape effect of quick-alignment particles has also been examined but no significant influence of shape is observed, which is due to the fact that active alignment is dominating and determines the swimming direction. The shape of particle affects the orientation through the fluid deformation rate and the shape effect is diminished due to the quick-alignment motility of particle. We, therefore, further explore the effects of particle shape and gravity in the case of slow-alignment particles in the following section.

3.2. Slow-alignment particles

In order to highlight the influence of particle shape on swimming strategies, we investigated slow-alignment particles with $v_{swim} = 0.3u_0$, $B = 5L_0/u_0$ and $v_s^{iso} = 0.1089u_0$. Under this circumstance, the term of active orientation is much smaller than that of quick-alignment particles studied in earlier section. Therefore, the flow plays a more important role in particle behaviour. Firstly, we consider particle without settlement. Figure 6 shows the instantaneous distributions of smart and naive particles with different aspect ratios. Both smart and naive particles show a stronger clustering as aspect ratio increases, which is the result of the decreased random distribution of orientation caused by non-zero local strain rate. Additionally, particles perform better with increasing aspect ratio (figure 7). The mean vertical velocities of both smart and naive particles increase with aspect ratio but saturated at aspect ratio larger than 10. The result indicates a possible relation between clustering and the ability of particles to travel upwards.

To further explore the connection between clustering and particle performance, the probability distribution functions of absolute vorticity at particle locations are shown in figure 8. Both smart and naive spherical particles distribute randomly in the flow without gravity, which is in accordance with the result of previous study (Durham *et al.* 2011; Colabrese *et al.* 2017). However, as the aspect ratio increases, both smart and

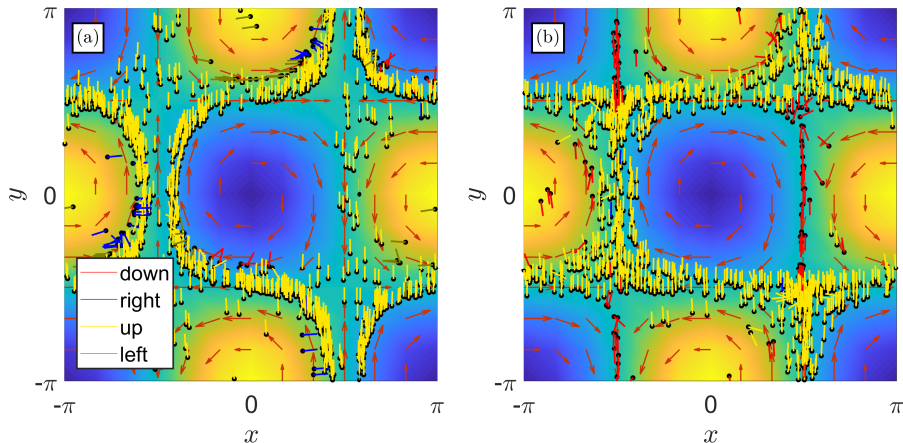


FIGURE 5. Instantaneous particle distribution of (a) non-settling particles and (b) settling particles. Black dots represent the positions of particles, and short lines represent the instantaneous orientation of particles, coloured by the preferential orientation. Red arrows indicate the local flow velocity.

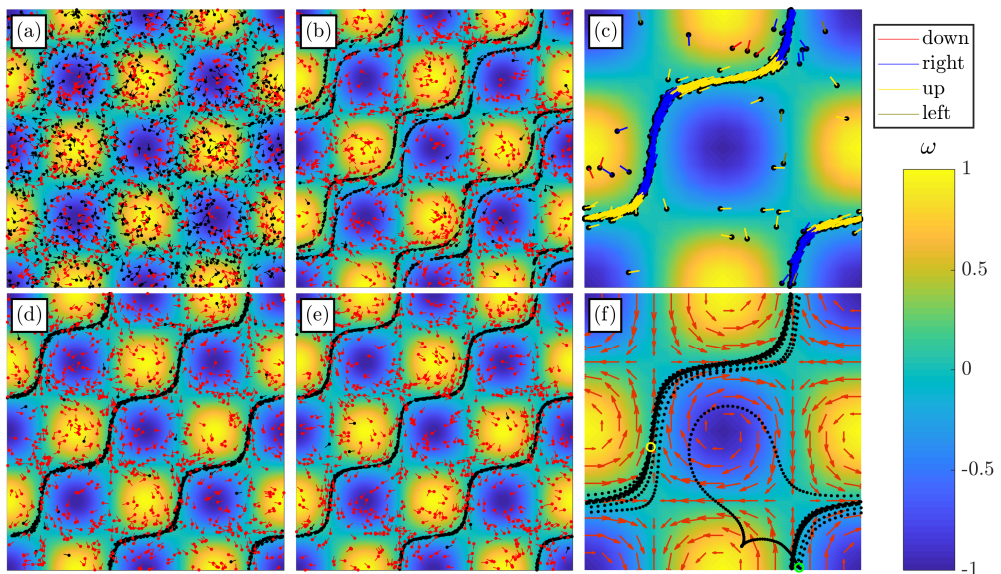


FIGURE 6. Instantaneous distribution of smart and naive non-settling particles with different aspect ratios in a $4\pi \times 4\pi$ domain. (a) $\lambda=1$, (b) $\lambda=2$, (d) $\lambda=3$, (e) $\lambda=5$. Black dots represent smart particles and red ones represent naive particles. (c) The instantaneous distribution and orientation of settling smart particles ($\lambda=3$) with tiny straight lines indicating the orientation vector \mathbf{p} coloured by its preferential alignment. (f) The typical trajectories of smart particles ($\lambda=3$), red arrows indicating local flow velocity. The green circle denotes the starting position while the yellow circle denotes the end position. Note that (e) and (f) are shown in a $2\pi \times 2\pi$ domain. The background is coloured by fluid vorticity.

naive particles gradually show a tendency to cluster at low vorticity regions. Moreover, figure 8 indicates that elongated particles preferentially sample upwelling region, while spherical particles tend to cluster in downward flow. It is noteworthy that the clustering pattern is consistent with the findings in turbulence, in which naive gyrotactic spheres

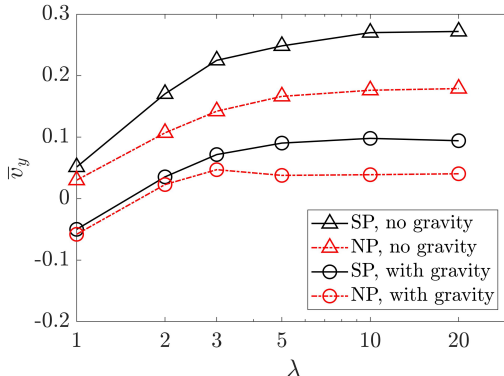


FIGURE 7. Mean vertical velocity of smart and naive particles in different case at last few episodes of training. Velocity averaged in $t=0$ 100. SP denotes smart particles while NP denotes naive particles.

sample downward flow while elongated spheroids sample upward flow (Borgnino *et al.* 2018; Gustavsson *et al.* 2016). Smart particles, however, show even stronger clustering and sampling in low vorticity and upwelling regions, and thus have better performance than naive particles. In our view, there are two mechanisms that lead to higher averaged vertical velocity of clustered particles. First, particles gathering between vortices avoid being trapped in or disturbed by vortices, which may drive particles rotating and prevent them from swimming in the specific direction. Second, the highest fluid velocity is located in the regions between vortices and the upward flow can lift particles upwards. Hence, by clustering between vortices and sampling upwelling flow, elongated particles can move upwards faster. Smart particles, which perform better than naive particles, successfully capture and exploit the feature of the background flow after being trained in the reinforcement learning process.

To better understand how particle swimming strategies capture the flow feature, we examined the contribution of active alignment (F_a), vorticity (F_Ω) and deformation rate (F_S) in particle rotational equation (figure 9).

$$F_a = \frac{1}{N_p} \sum_{n=1}^{N_p} \left| \frac{1}{2B} [\mathbf{k}_a - (\mathbf{k}_a \cdot \mathbf{p}) \mathbf{p}] \right|_n, \quad (3.1)$$

$$F_\Omega = \frac{1}{N_p} \sum_{n=1}^{N_p} \left| \frac{1}{2} \boldsymbol{\omega} \times \mathbf{p} \right|_n, \quad (3.2)$$

$$F_S = \frac{1}{N_p} \sum_{n=1}^{N_p} \left| \frac{\lambda^2 - 1}{\lambda^2 + 1} [\mathbf{I} - \mathbf{p}\mathbf{p}] \mathbf{S}\mathbf{p} \right|_n, \quad (3.3)$$

where N_p is the total number of particles simulated. When particles are randomly distributed in the flow field initially, vorticity is dominant on particles alignment. However, the smart particles quickly react to the background flow and start to get away from vortex, which is illustrated by the decreasing F_Ω and increasing F_S in figure 9. By contrast, naive particles don't show obvious clustering. We found that smart particles are able to swim to the regions between vortices and with an upward flow motion under the instruction of swimming strategy, and then be driven upwards by the flow (see figure 6c, f). In such regions, particle orientation is dominated by local strain rate of the flow,

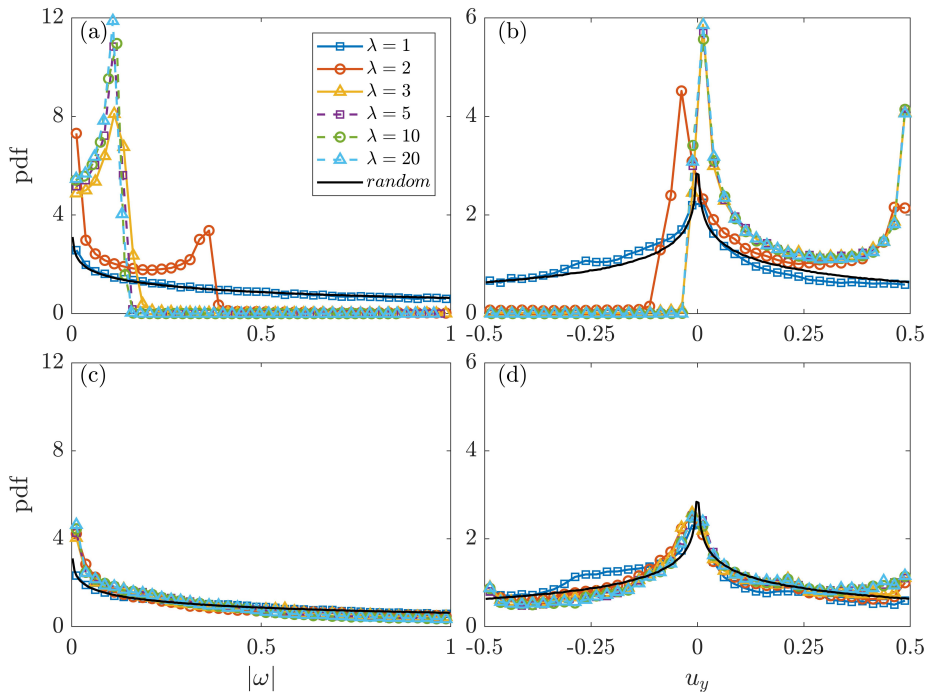


FIGURE 8. The probability distribution function of absolute vorticity (a, c) and vertical flow velocity (b, d) at (non-settling) particle locations. (a, b) Smart particles; (c, d) naive particles.

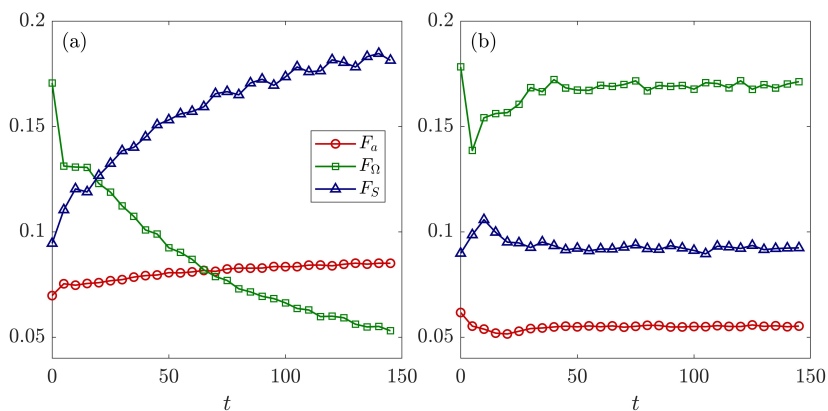


FIGURE 9. The mean contribution of active alignment F_a , vorticity F_Ω and deformation rate F_S changes over time. (a) Smart particles; (b) naive particles. $\lambda=3$, no gravity.

which drives particles aligning horizontally or vertically. However, particles keep trying to rotate themselves to the preferential orientation which is perpendicular to their current orientation as shown in figure 6c. The balance between the hydrodynamic effect of fluid and the active alignment of particle determines the orientation, explaining the winding track shown in figure 6. Strategies help particles correct their swimming direction and keep them on the right track by changing preferred orientation based on state of particles (figure 6c). Thus, a moderate level of F_a is seen in figure 9. Once a particle is accidentally thrown away from the track, it is able to swim back on the track under the swimming strategy (see figure 6f).

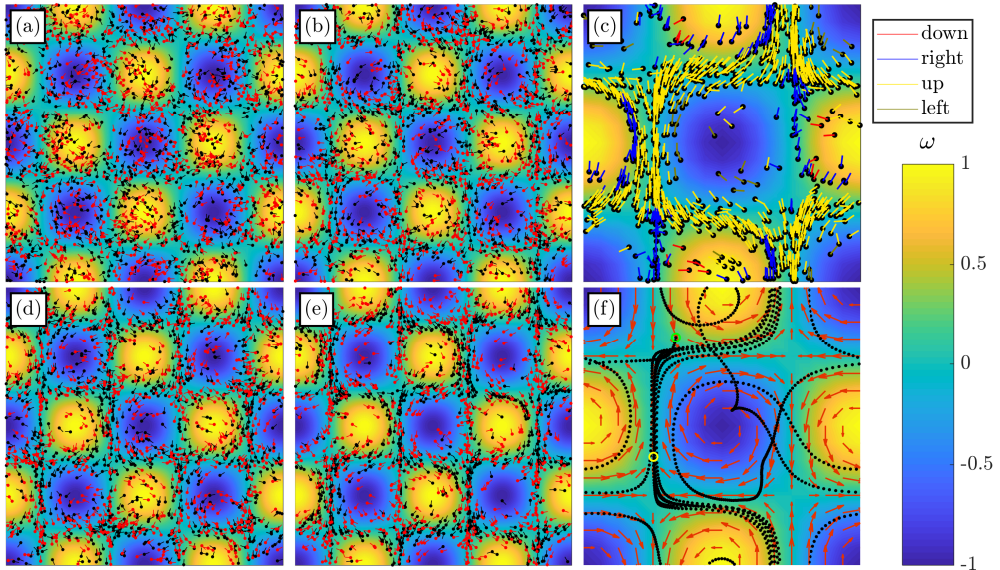


FIGURE 10. Instantaneous distribution of smart and naive settling particles with different aspect ratios in a $4\pi \times 4\pi$ domain. (a) $\lambda=1$, (b) $\lambda=2$, (d) $\lambda=3$, (e) $\lambda=5$. Black dots represent smart particles and red ones represent naive particles. (c) The instantaneous distribution and orientation of settling smart particles ($\lambda=3$) with tiny straight lines indicating the orientation vector p coloured by its preferential alignment. (f) The typical trajectories of smart particles ($\lambda=5$), red arrows indicating local flow velocity. The green circle denotes the starting position while the yellow circle denotes the end position. Note that (e) and (f) are shown in a $2\pi \times 2\pi$ domain. The background is coloured by fluid vorticity.

When gravity is applied on slow-alignment particles, clustering becomes much weaker than the cases without gravity (figure 10). The clustering patterns of smart and naive particles are found to be similar (figure 11) and smart particles only slightly outperform naive particles at aspect ratio less than 3 (figure 7). Although settling particles swim upwards faster as aspect ratio increases, a plateau of the averaged vertical velocity is observed at aspect ratio larger than 3, which indicates the vanishing shape effect on the efficiency of swimming upwards. The significant settling velocity, in our view, prevents particles from travelling steadily on the track. Particles need to orientate upwards and swim against the gravity to prevent falling into vortices, which results in a strategy that particles orientate upwards in most the regions of flow (figure 10c). Smart particles, therefore, exhibit similar clustering pattern to the naive gyrotactic particles. The similarity between elongated smart particles and naive particles under more realistic constraints is interesting and we hypothesize that the naive gyrotactic particle model might be an almost optimal swimming strategy in more realistic flow environment. This hypothesis is deserved to be investigated in further study of smart particles in turbulence.

4. Concluding Remarks

Earlier studies (Colabrese *et al.* 2017; Gustavsson *et al.* 2017; Colabrese *et al.* 2018) succeeded in finding efficient swimming strategies for spherical particles in flow fields, but excluded the effect of settlement and aspherical shape of particles. However, these two effect is commonly observed in reality, which might be influential to swimming strategy

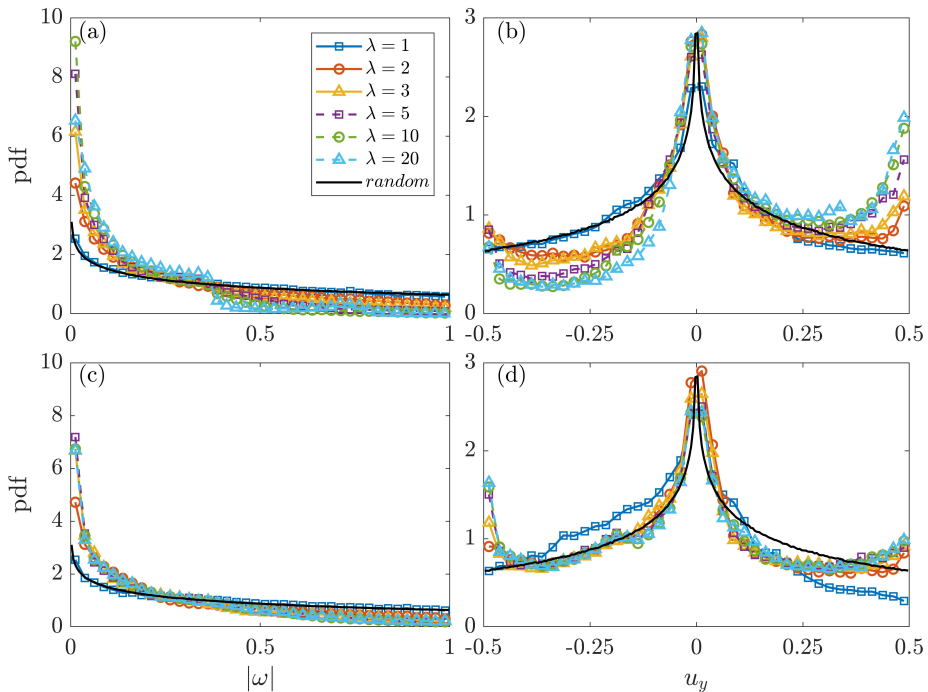


FIGURE 11. The probability distribution function of absolute vorticity (a, c) and vertical flow velocity (b, d) at (settling) particle locations. (a, b) Smart particles; (c, d) naive particles.

of microorganisms. Therefore, we present an investigation on swimming strategy of non-spherical settling particles in a TGV flow using reinforcement learning approach.

In the case of quick-alignment particles, three different solutions of swimming strategy are obtained when gravity is neglected, indicating that multi-solutions of strategy are given by reinforcement learning. However, only one type of strategy with the best performance is obtained when gravity is considered. We conclude that the convergence of multi-solutions could be reached when particle motion is more constrained (e.g. being influenced by gravity or having weaker motility). The further investigation on specific actions of swimming direction in downwelling region for a slower-swimming particles also supports this statement. Non-settling particles can swim upwards or downwards with the same level of rewards. Therefore, both actions are observed in several strategies that are separately trained. For settling particles, however, an interesting phenomenon is observed that in all strategies particles sacrifice the short-term reward to swim downwards in downwelling flow in order to quickly get rid of the unprofitable region and pursue a higher long-term reward.

We also consider slow-alignment particles to highlight the shape effect on swimming strategies. The results of non-settling particles suggest that the elongation of smart and naive particles enhances the efficiency of swimming upwards, but smart particles trained by reinforcement learning approach clearly move faster than naive ones. We reveal that the advancement of smart particles is achieved by enhancing the clustering in low vorticity and upwelling region by the active choice of preferential orientation. However, with inclusion of gravity, the efficiency of swimming upward is attenuated for both smart and naive particles. Smart particles only slightly outperform naive ones and the improvement is attenuated at small aspect ratio. Elongated particles have better performance than spheres, but no obvious enhancement is observed at aspect ratio

larger than three. Moreover, we discover that smart particles at aspect ratio smaller than three behave similarly to naive ones in presence of gravity effect. In other words, smart particles align and swim upwards more often to resist the significant settling. Such observation leads to a conjecture that the elongated shape and the gyrotaxis of a particle may be an almost optimal strategy for swimming upwards against gravity. Combined with the finding that additional constraints restrict the multi-solutions of strategy, it is natural to suspect that the elongation and the gyrotaxis of microorganisms is a simple but efficient strategy evolved through natural selection in aquatic environment, such as oceanic flows. On the other hand, the similar behaviour of smart and naive particle under more realistic conditions exhibit the effectiveness of reinforcement learning approach. Therefore, reinforcement learning approach might be a tool with great potential to study the microorganisms in realistic flow environment.

Acknowledgements

The authors are grateful for the support of Natural Science Foundation of China through grants nos. 11702158 and 91752205. Sigma2 is acknowledged for the support of computational resources through grant no. NN2694K (Program for Supercomputing) of the Research Council of Norway.

Appendix A.

As mentioned in Section 2, we are also interested in accelerating the training process of reinforcement learning. The Appendix provides a detailed comparison of training with a single particle and multiple particles. Both types of training are processed under the same operation conditions ($v_{swim} = 0.3$, $B = 5L_0/u_0$, $\lambda = 3$, learning rate $\alpha = 0.2$ and all initial elements of Q table are 5000). The only difference is the particle number. One hundred particles are used simultaneously in the training procedure in multiple-particle case, while only one particle is trained in single-particle case. Figure 12 shows the learning gains and both cases reach a similar level of final learning gain (more precisely, the gain obtained by multiple-particle approach is only about 5-10% lower). The results reveal that multiple-particle training is working fine considering the similar performance of strategy obtained in present work. In our view, particles have experienced sufficient state changes since one hundred particles are initialized with random distribution in every episode, which leads to adequate explorations. Moreover, the update of Q table is more frequent in multiple-particle case. Therefore, the number of episodes needed to converge in approximately optimal strategies is only around 400 for multiple-particle training, while the episode number of single-particle case is around 40 000. Although the computation cost of each episode is higher in multiple-particle training, the total time cost is greatly reduced because the motion of multiple particles can be solved in parallel. The degree of efficiency improvement depends on the learning rate and particles number trained at the same time, which should be chosen according to the specific problem. In the present work, for instance, the time cost of a single episode of training one hundred particles is about four times higher than the training of single particle. However, considering the 99% reduction of episode number, the estimated total time cost of multiple-particle training is only about 4% of single-particles case.

The computation cost of training may become a bottleneck in the simulations of complex flow configurations, such as turbulent flow or finite size particles laden flow. Therefore, with appropriate parameters, adopting multiple-particle training approach is

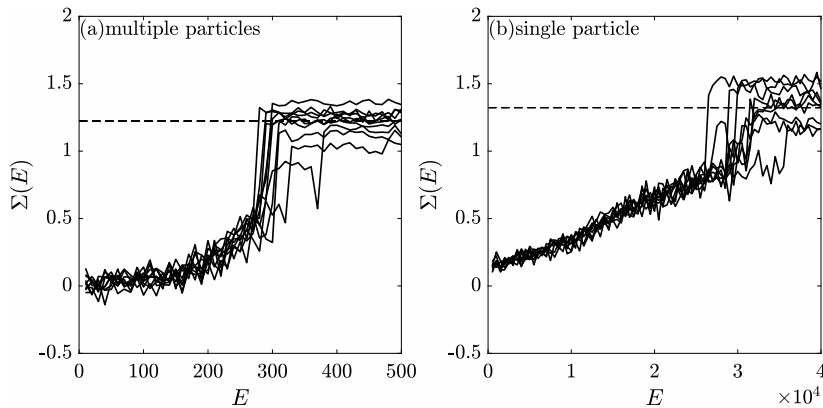


FIGURE 12. Learning gains of (a) multiple-particle case and (b) single-particle case. The values are averaged every 10 episodes in multiple particles case and 500 episodes in single particle case. Black dashed line represents the averaged value of 10 independent trainings.

useful to reduce the training cost and increase the feasibility of application of reinforcement learning approach.

REFERENCES

- BEARON, R. N., HAZEL, A. L. & THORN, G. J. 2011 The spatial distribution of gyrotactic swimming micro-organisms in laminar flow fields. *J. Fluid Mech.* **680**, 602–635.
- BLAIR, D. F. 1995 How bacteria sense and swim. *Annu. Rev. Microbiol.* **49** (1), 489–520.
- BORGNO, M., BOFFETTA, G., DE LILLO, F. & CENCINI, M. 2018 Gyrotactic swimmers in turbulence: shape effects and role of the large-scale flow. *J. Fluid Mech.* **856**, R1.
- COLABRESE, S., GUSTAVSSON, K., CELANI, A. & BIFERALE, L. 2017 Flow navigation by smart microswimmers via reinforcement learning. *Phys. Rev. Lett.* **118** (15), 158004.
- COLABRESE, S., GUSTAVSSON, K., CELANI, A. & BIFERALE, L. 2018 Smart inertial particles. *Phys. Rev. Fluids* **3** (8), 084301.
- CROZE, O. A., SARDINA, G., AHMED, M., BEES, M. A. & BRANDT, L. 2013 Dispersion of swimming algae in laminar and turbulent channel flows: consequences for photobioreactors. *J. Royal Soc. Interface* **10** (81).
- DE LILLO, F., CENCINI, M., DURHAM, W. M., BARRY, M., STOCKER, R., CLIMENT, E. & BOFFETTA, G. 2014 Turbulent fluid acceleration generates clusters of gyrotactic microorganisms. *Phys. Rev. Lett.* **112** (4), 044502.
- DRESCHER, K., LEPTOS, K. C., TUAL, I., ISHIKAWA, T., PEDLEY, T. J. & GOLDSTEIN, R. E. 2009 Dancing volvox: hydrodynamic bound states of swimming algae. *Phys. Rev. Lett.* **102** (16), 168101.
- DURHAM, W. M., CLIMENT, E. & STOCKER, R. 2011 Gyrotaxis in a steady vortical flow. *Phys. Rev. Lett.* **106**, 238102.
- DURHAM, W. M., KESSLER, J. O. & STOCKER, R. 2009 Disruption of vertical motility by shear triggers formation of thin phytoplankton layers. *Science* **323** (5917), 1067–1070.
- FUCHS, H. L., GERBI, G. P., HUNTER, E. J., CHRISTMAN, A. J. & DIEZ, F. J. 2015 Hydrodynamic sensing and behavior by oyster larvae in turbulence and waves. *J. Exp. Biol.* **218** (9), 1419–1432.
- FUCHS, H. L., HUNTER, E. J., SCHMITT, E. L. & GUAZZO, R. A. 2013 Active downward propulsion by oyster larvae in turbulence. *J. Exp. Biol.* **216** (8), 1458–1469.
- GARCIA, X., RAFA, S. & PEYLA, P. 2013 Light control of the flow of phototactic microswimmer suspensions. *Phys. Rev. Lett.* **110** (13), 138106.
- GAZZOLA, M., TCHIEU, A. A., ALEXEEV, D., DE BRAUER, A. & KOUMOUTSAKOS, P. 2016 Learning to school in the presence of hydrodynamic interactions. *J. Fluid Mech.* **789**, 726–749.

- GUSTAVSSON, K., BERGLUND, F., JONSSON, P. R. & MEHLIG, B. 2016 Preferential sampling and small-scale clustering of gyrotactic microswimmers in turbulence. *Phys. Rev. Lett.* **116** (10), 108104.
- GUSTAVSSON, K., BIFERALE, L., CELANI, A. & COLABRESE, S. 2017 Finding efficient swimming strategies in a three-dimensional chaotic flow by reinforcement learning. *Eur. Phys. J. E* **40** (12), 110.
- KESSLER, J. O. 1985 Hydrodynamic focusing of motile algal cells. *Nature* **313** (5999), 218–220.
- KESSLER, J. O. 1986*a* The external dynamics of swimming micro-organisms. *Prog. Phycol. Res.* **4**, 258–307.
- KESSLER, J. O. 1986*b* Individual and collective fluid dynamics of swimming cells. *J. Fluid Mech.* **173**, 191–205.
- NAIAZI ARDEKANI, M., SARDINA, G., BRANDT, L., KARP-BOSS, L., BEARON, R. N. & VARIANO, E. A. 2017 Sedimentation of inertia-less prolate spheroids in homogenous isotropic turbulence with application to non-motile phytoplankton. *J. Fluid Mech.* **831**, 655–674.
- NOVATI, G., VERMA, S., ALEXEEV, D., ROSSINELLI, D., VAN REES, W. M. & KOUMOUTSAKOS, P. 2017 Synchronisation through learning for two self-propelled swimmers. *Biomim.* **12** (3), 036001.
- PEDLEY, T. J. & KESSLER, J. O. 1987 The orientation of spheroidal microorganisms swimming in a flow field. *Proc. Royal Soc. Lond.* **231** (1262), 47–70.
- PEDLEY, T. J. & KESSLER, J. O. 1992 Hydrodynamic phenomena in suspensions of swimming microorganisms. *Annu. Rev. Fluid Mech.* **24** (1), 313–358.
- POFF, K. L. & SKOKUT, M. 1977 Thermotaxis by pseudoplasmodia of dictyostelium discoideum. *P. Natl Acad. Sci. Usa* **74** (5), 2007–2010.
- REDDY, G., CELANI, A., SEJNOWSKI, T. J. & VERGASSOLA, M. 2016 Learning to soar in turbulent environments. *Proc. Natl. Acad. Sci. U.S.A.* **113** (33), E4877–E4884.
- SANTAMARIA, F., DE LILLO, F., CENCINI, M. & BOFFETTA, G. 2014 Gyrotactic trapping in laminar and turbulent kolmogorov flow. *Phys. Fluids* **26** (11), 111901.
- SENGUPTA, A., CARRARA, F. & STOCKER, R. 2017 Phytoplankton can actively diversify their migration strategy in response to turbulent cues. *Nature* **543** (7646), 555–558.
- SIEWERT, C., KUNNEN, R. P. J., MEINKE, M. & SCHRDER, W. 2014 Orientation statistics and settling velocity of ellipsoids in decaying turbulence. *Atmos. Res.* **142**, 45–56.
- SUTTON, R. S. & BARTO, A. G. 1998 *Reinforcement learning: An introduction (Adaptive computation and machine learning)*. Cambridge: MIT Press.
- TAWADA, K. & MIYAMOTO, H. 1973 Sensitivity of paramecium thermotaxis to temperature change. *J. Eukaryot. Microbiol.* **20** (2), 289–292.
- THORN, GRAEME J. & BEARON, RACHEL N. 2010 Transport of spherical gyrotactic organisms in general three-dimensional flow fields. *Phys. Fluids* **22** (4), 041902.
- ZHAN, C., SARDINA, G., LUSHI, E. & BRANDT, L. 2014 Accumulation of motile elongated micro-organisms in turbulence. *J. Fluid Mech.* **739**, 22–36.